Supplementary Figure S4

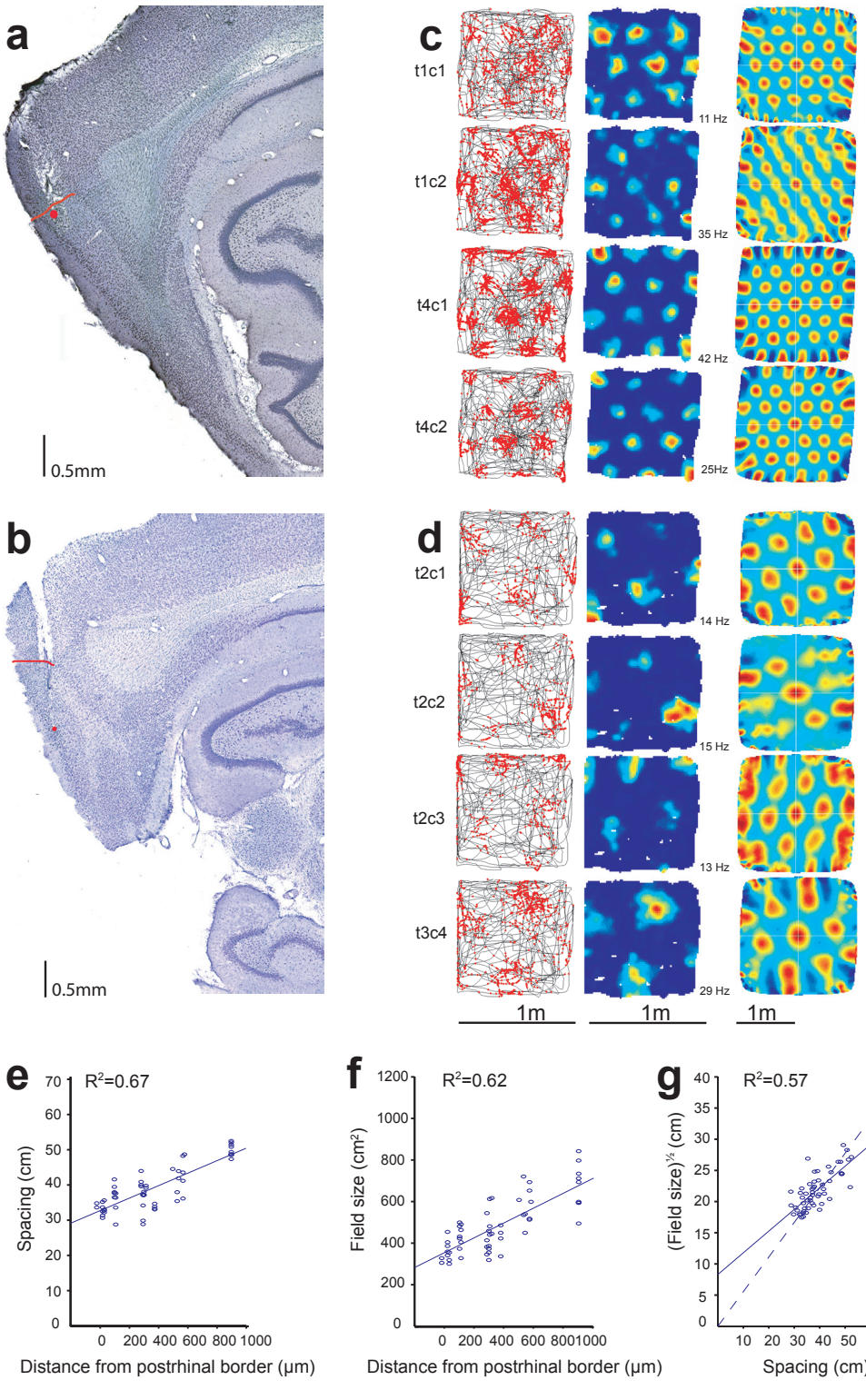

Topographic organization of grid cells. **ab**, Sagittal sections indicating extreme recording locations in dorsal **(a)** and ventral **(b)** dMEC (red circles). The dorsal position was near the postrhinal cortex (red line); the ventral position was 900 µm deeper. **bd**, Colour-coded firing rate maps showing denser spacing at the dorsal position **(c)** than at the ventral position **(d)** during running in a square enclosure (1 m X 1 m). Note that spacing and orientation were constant between cells at the same location. **ef**, Grid spacing **(e)** and size of fields at the grid vertices **(f)** as a function of the distance between the electrodes and the postrhinal border (all animals). Regression lines are indicated. The distance from the postrhinal border correlated significantly with the spacing of the grid ($r(55) = 0.82$, $P < 0.001$, with cells as the unit of analysis; $r(9) = 0.76$, $P < 0.01$, with rats as the unit of analysis). Distance from the postrhinal border also correlated with the size of the individual fields (cells as unit: $r = 0.79$, $P < 0.001$; rats as unit: $r = 0.90$, $P < 0.001$). **g**, Isometric relation between spacing and field size. Dashed line shows regression through the origin. Regression through the origin yielded a better Bayesian Information Criterion (Schwartz criterion) score (263 without intercept vs. 245 with intercept), indicating that field spacing and field radius scale proportionally along the dorsoventral axis of dMEC.